Supplementary Information

Shape-Memory Effect in an Organosuperelastic Crystal

Satoshi Takamizawa and Yuichi Takasaki*

Department of Nanosystem Science; Graduate School of Nanobioscience;
Yokohama City University; 22-2 Seto; Kanazawa-ku,
Yokohama, Kanagawa 236-0027; Japan
staka@yokohama-cu.ac.jp

Contents:

Other materials:

Movie S1: Thermal shape-recovery motion (Video for Fig. 1 a-c)
Movie S2: Twinning and superelastic motion (Video for Figs. 3 d & e)
Movie S3: Thermal heavy-lifting work (Video for Fig. 7)

Crystal Structures

Table S1. Single-Crystal data for **1**.

Pphase	α	α	α	β
T /K	183	298	394	403
Empirical formula	$C_{40}H_{56}BP$	$C_{40}H_{56}BP$	$C_{40}H_{56}BP$	$C_{40}H_{56}BP$
Crystal size /mm^3	0.35×0.09×0.09	0.75×0.16×0.09	0.46×0.14×0.11	1.00×0.24×0.23
M	578.63	578.63	578.63	578.63
Crystal system	Triclinic	Triclinic	Triclinic	Monoclinic
Space group	*P*-1	*P*-1	*P*-1	$P2_1/n$
a /Å	10.1868(7)	10.311(3)	10.5582(11)	12.1401(14)
b /Å	18.7141(13)	18.895(5)	19.131(2)	36.975(4)
c /Å	20.7566(15)	20.770(6)	20.915(2)	17.688(2)
α /deg	70.748(2)	69.618(7)	68.892(2)	90
β /deg	86.972(2)	85.946(7)	85.501(3)	102.611(2)
γ /deg	76.006(2)	76.898(6)	77.175(2)	90
V /Å^3	3623.3(4)	3694.1(18)	3842.7(7)	7748.1(15)
Z	4	4	4	8
D_{calcd} / Mg m^{-3}	1.061	1.040	1.000	0.992
μ(Mo Kα) / mm^{-1}	0.101	0.099	0.095	0.094
Reflections collected	21308	21495	22471	57189
Independent reflections (R_{int})	12760(0.0799)	12972(0.0459)	13522(0.0410)	19194(0.0892)
Goodness of fit	1.004	1.120	0.894	1.123
R_1(I > 2σ (all data))	0.0888(0.2179)	0.1120(0.2319)	0.0960(0.2774)	0.1668(0.4430)
wR_2(I > 2σ (all data))	0.1966(0.2639)	0.3496(0.4207)	0.2660(0.3982)	0.4463(0.5654)
Largest diff. peak (hole) /eÅ^3	0.724(-0.349)	0.443(-0.336)	0.421(-0.264)	0.476(-0.265)

CCDC numbers: 1422938 (α phase at 183K), 986256 (α phase at 298 K), 986257 (α phase at 394 K), and 986258 (β phase at 403 K).

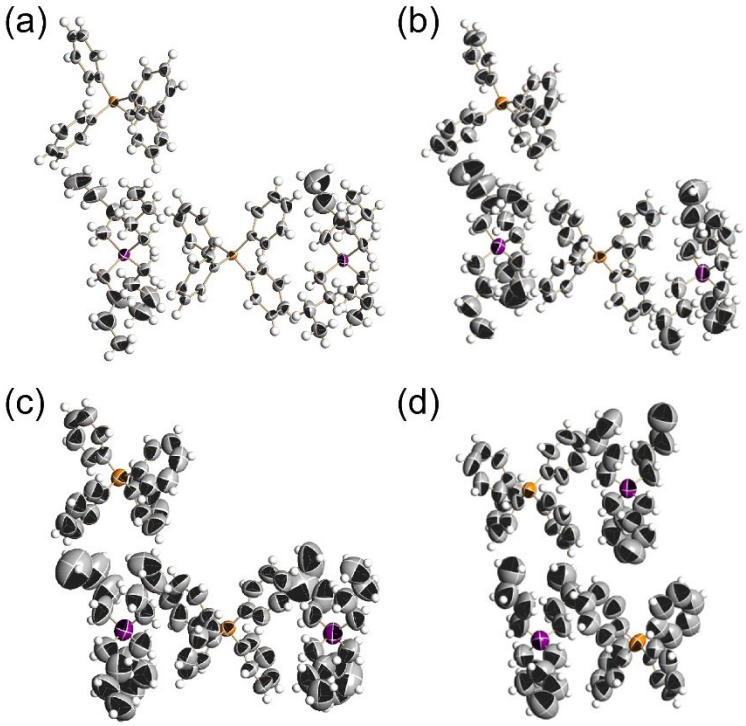

Figure S1. Thermal ellipsoid drawing of **1** at the 50% probability level: (a) α phase at 183 K, (b) α phase at 298 K, (c) α phase at 394 K, and (d) β phase at 403 K. Elements are color coded: C (gray), H (white), B (orange), and P (purple).

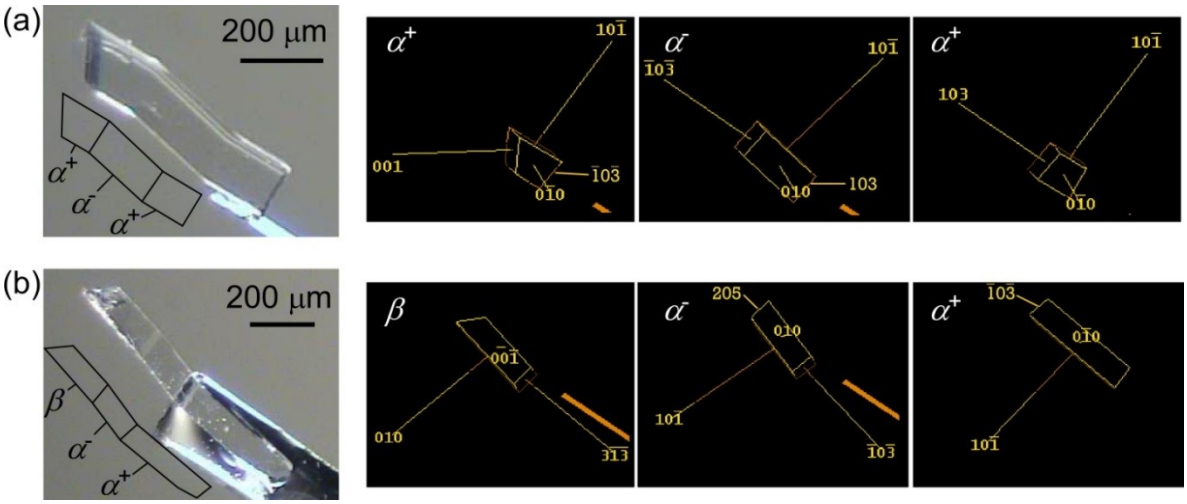

Figure S2. Crystal surface indexes of **1** under the following conditions: α^+/α^- twinning at 298K (a) and $\beta/\alpha^-/\alpha^+$ deformed state at 394.6 K (=121.6 °C) (M_s, 120.46 °C; A_s, 123.00 °C) (b).

Thermal Analysis

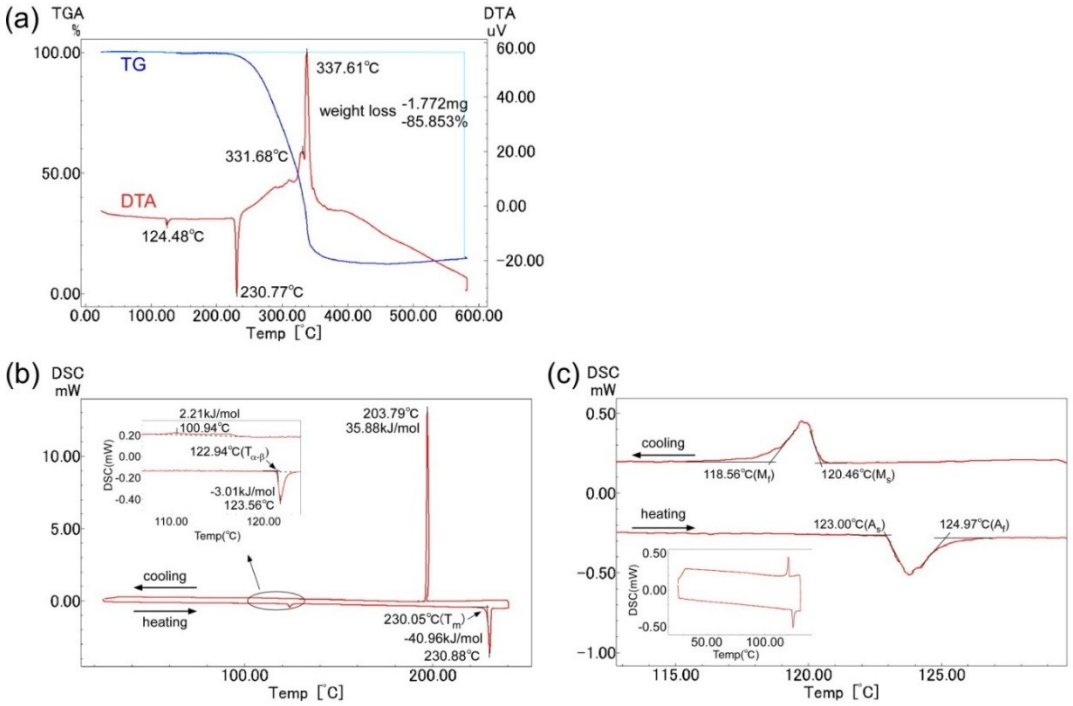

Figure S3. DTG (a) and DSC (b, c) charts for **1**. Chart (c) is a magnification to clarify the transition region in (b). (Temperature rate: 5 K min^{-1} in DTG and 2 K min^{-1} in DSC) The important thermodynamic parameters are summarized in Table 1.

Powder X-ray Diffraction Measurements

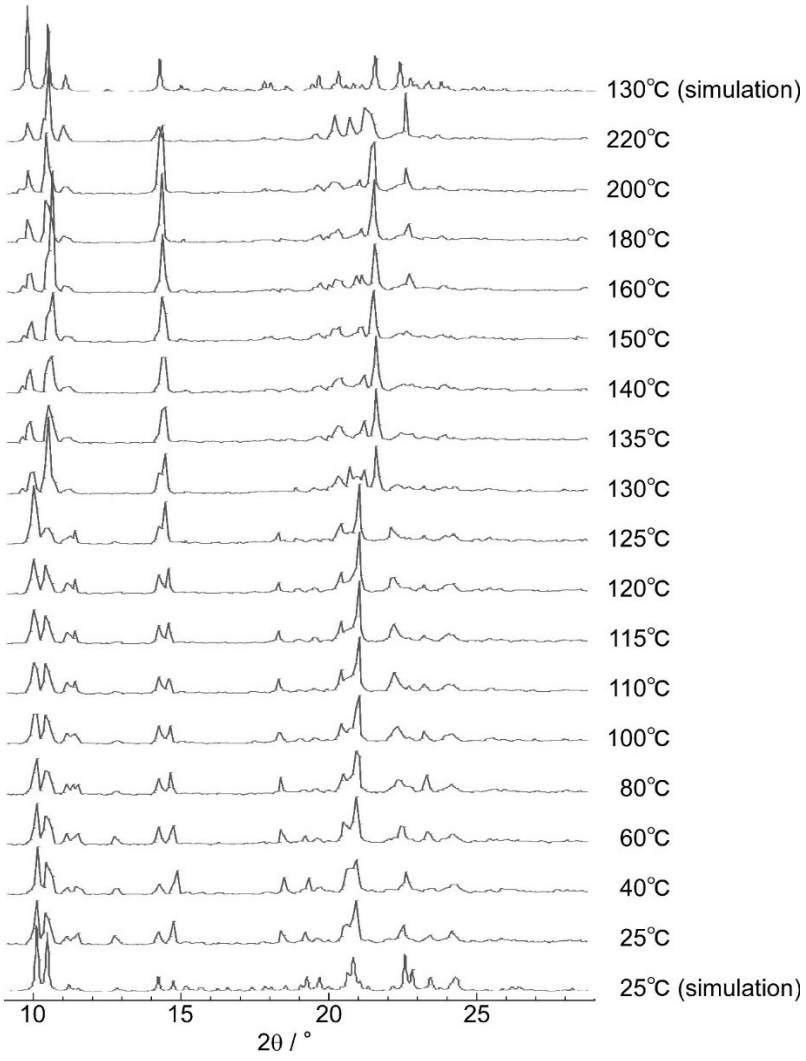

Figure S4. Powder X-ray diffraction patterns of **1** heated from 25 °C to 220 °C. (Height of the patterns indicate a relative intensity. Top and bottom patterns are simulations from single-crystal X-ray diffraction data at 25 °C and 130 °C.) Change of the patterns around 125 °C agrees with the transition temperature of A_s (123.00 °C) or A_f (124.97 °C) obtained from the DSC measurements.

Transfer Velocity of α-β Interface

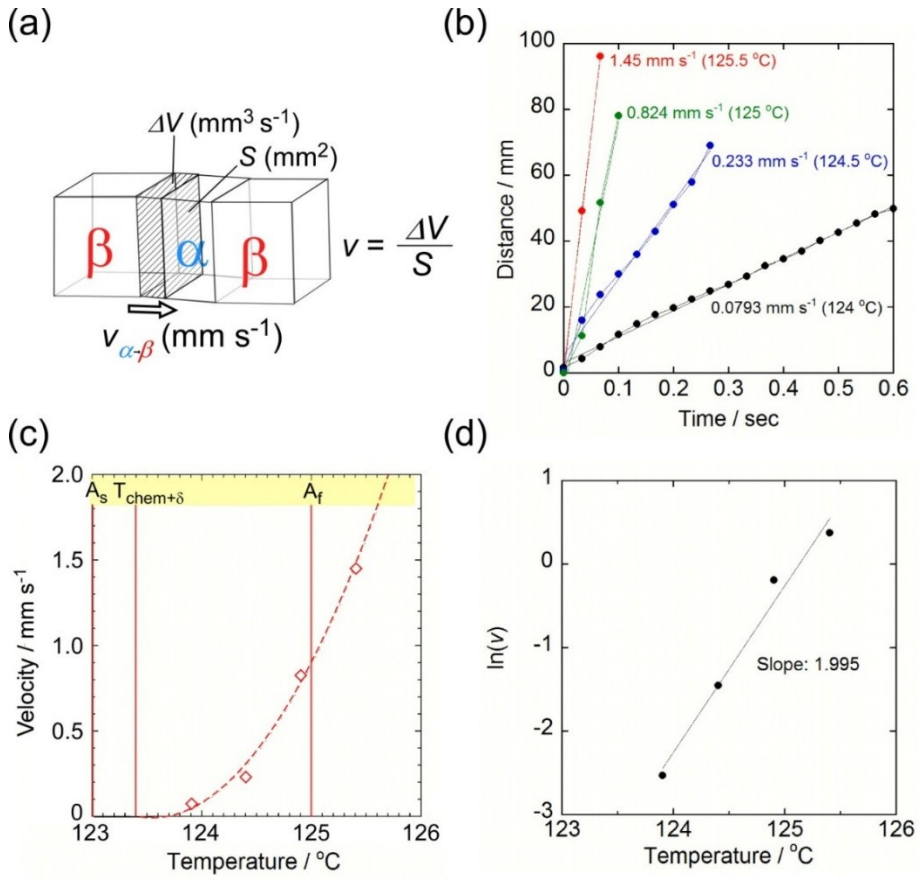

Figure S5. Temperature dependence of the velocity of α/β interface in diminishing α phase during spontaneous α→β transformation. Definition of velocity of α-β interface transfer (a); time course of α-β interface displacement in spontaneous reverse transformation in retracting the pushing blade on the $(0\text{-}10)_{\beta}$ face at 124 °C (black), 124.5 °C (blue), 125 °C (green), and 125.5 °C (red) (b); square proportion of velocity to temperature (c); determination of multiplier (=2) by the least squares method on logarithmic plot (d).

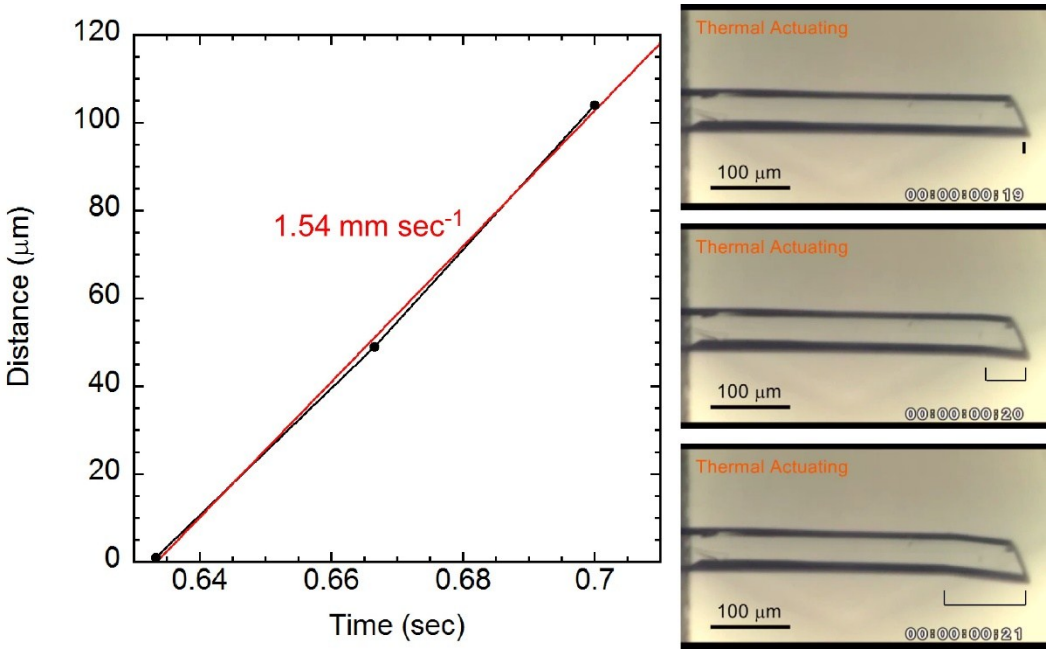

Figure S6. The observed velocity of interface transfer was 1.54 mm sec^{-1} in the experiment (150 °C heat source). (Nose of electric iron rocking by hand under a microscope appeared on Fig. 1b in the paper although the velocity should depend on the way of heat regulation.)

Stress-Strain Test and Its Temperature Dependence

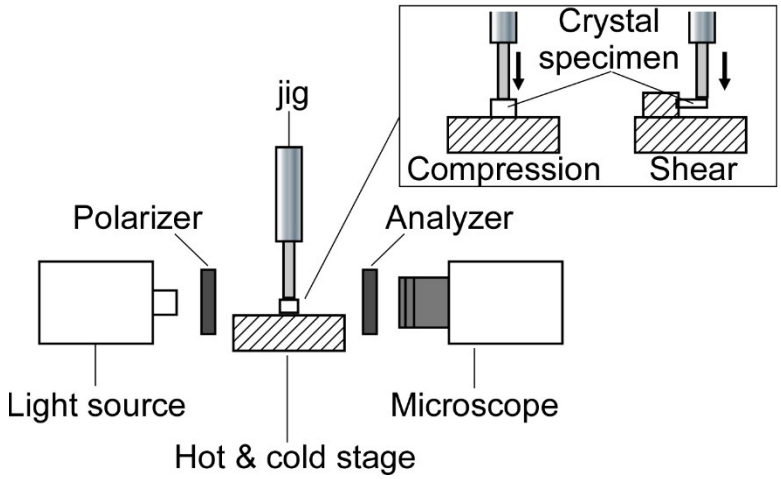

Figure S7. A set-up for stress-strain measurements on a universal testing machine with a temperature controlling system.

Table S2. Conditions of cyclic shear test on crystal **1**.

Temperature/ °C	Loading surface	Crystal dimension		Press type		Displacement velocity/ μm min^{-1}	Correspondence
		Width/ μm	Thicknes s/ μm	Contact area/ m^2	Jig (width / μm)		
-50~20	(10)	201	138	1.91×10^{-8}	Blade (95)	200	Fig. 3a, Fig. S8
40~120	(10)	111	161	1.05×10^{-8}	Blade (95)	200	Fig. 3a, Fig. S8
123.5~126.5	(010)	44	191	2.2×10^{-10}	Blade (5)	200	Fig. 3b, Fig. S8
119.5~123.2	(10)	201	105	1.91×10^{-8}	Blade (95)	200	Fig. S9a (blue)
123.1~124.6	(010)	111	161	5.6×10^{-10}	Blade (5)	200	Fig. S9a (red)
123.4~129.4	(010)	166	139	8.3×10^{-10}	Blade (5)	200	Fig. S9b
124.5	(010)	127	172	6.4×10^{-10}	Blade (5)	500	Fig. S10

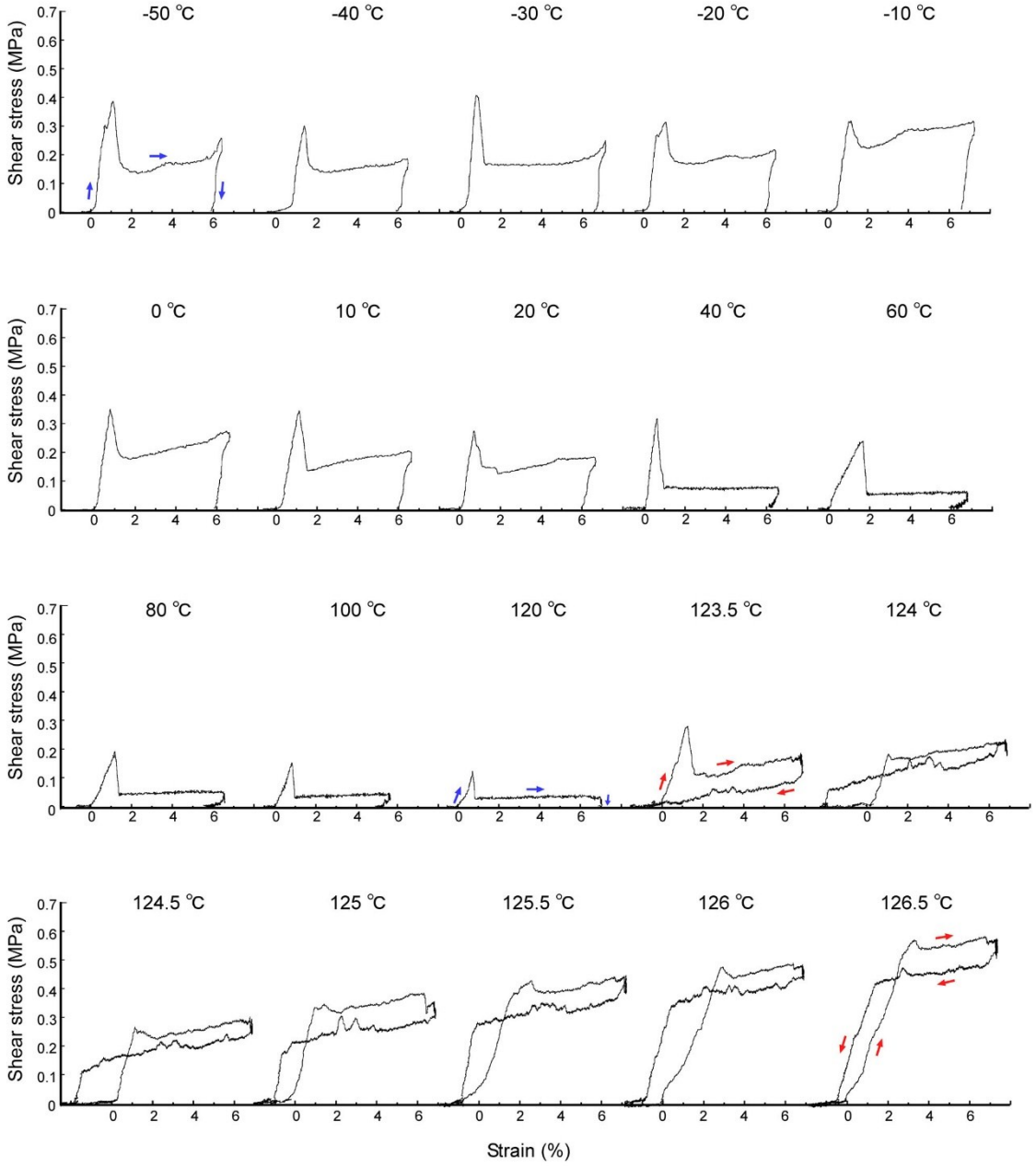

Figure S8. Stress-strain curves for all temperatures by using the single-crystal specimens listed in Table S2. (-50~120 °C: twinning transformations; 123.5~126.5 °C: superelastic transformations.)

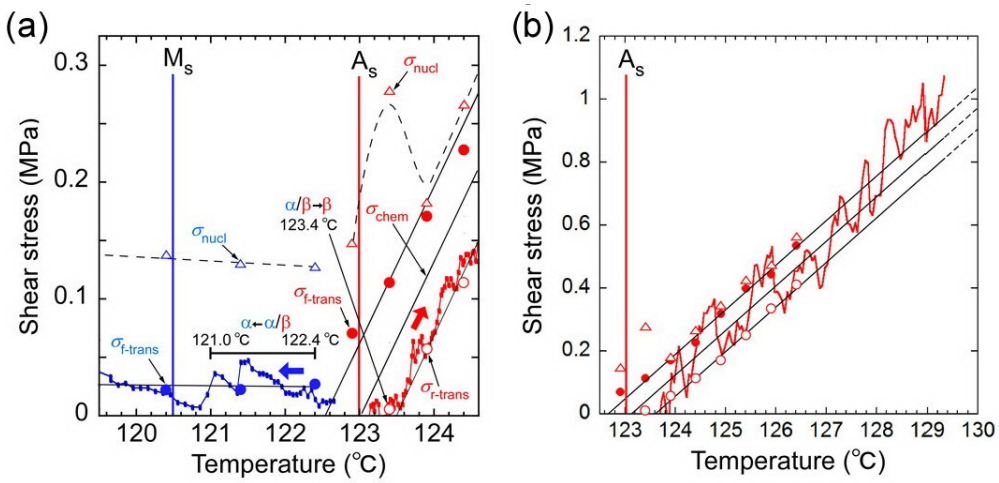

Figure S9. Trace of induced shear by mere temperature transition of **1** (blue and red plots indicate stressed crystal phase for α and β, respectively) around A_s (a) and higher temperature region (b). An α/β deformed state was preserved by jig contact with the detection limit level of force between T_{chem} (A_s) and $T_{chm+\delta}$. The static α/β transformed into α from 122.4 °C to 121.0 °C with an induced shear of about 0.03 (0.01-0.05) MPa in cooling (blue line) and began transformation into β at 123.4 °C with an induced shear of about 0.01 (0.005-0.01) MPa in warming before the $\sigma_{r\text{-}trans}$ generated with superelasticity (red line).

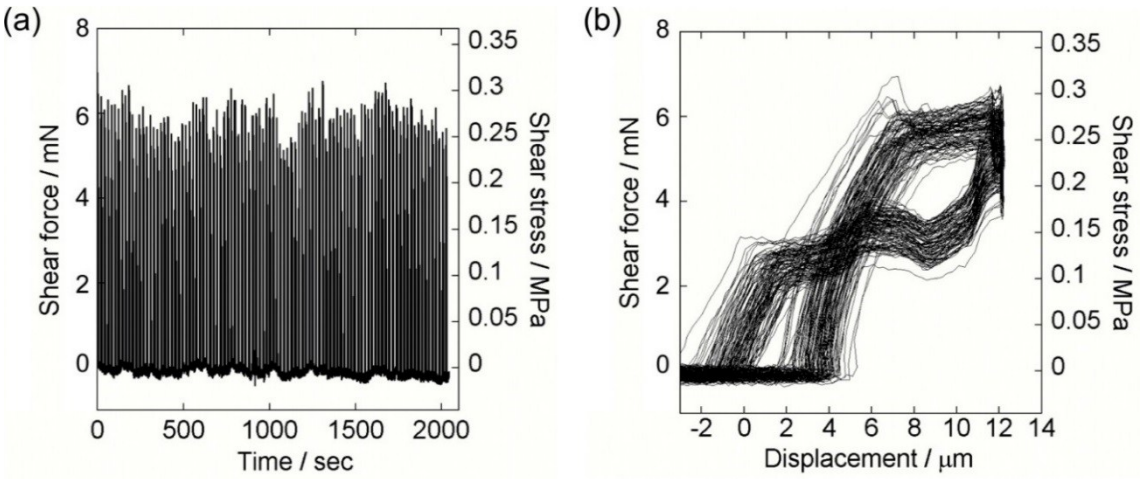

Figure S10. 100 cycles against time (a) and displacement (b) in shearing **1** at 124.5 °C.

Principal Indexes for Superelasticity of 1

The representative indexes changed from 3.7 to 26.5 kJ m^{-3} by energy density, from 0.06 to 0.77 by energy efficiency, and from 0.07 to 0.06 through 0.083 (124.5 °C) by superelastic index as the temperature changed from 123.5 °C to 126.5 °C. (Table S3, Fig. S11)

Table S3. Principal indexes of superelasticity of **1** at various temperatures.*

Temperature (°C)	Energy density (ρ) (kJ m^{-3}) [(J g^{-1})]	Energy efficiency (η)	Superelastic index (χ)
123.5	3.68 [0.00371]	0.0556	0.0681
124	9.19 [0.00926]	0.333	0.0808
124.5	14.2 [0.0143]	0.500	0.0832
125	18.9 [0.0191]	0.536	0.0773
125.5	21.6 [0.0218]	0.629	0.0666
126	21.9 [0.0221]	0.756	0.0562
126.5	26.5 [0.0267]	0.766	0.0561

*Crystal density is 0.992 Mg m^{-3}, which was given by X-ray data for β phase crystal of **1** at 403.0 K. ($\rho=W_{r\text{-}trans}/V_{f\text{-}trans}$; $\eta=W_{r\text{-}trans}/W_{f\text{-}trans}$; $\chi=\rho/\sigma_{chem}$: W means work input (f-trans) or output (r-trans) during transformation.)

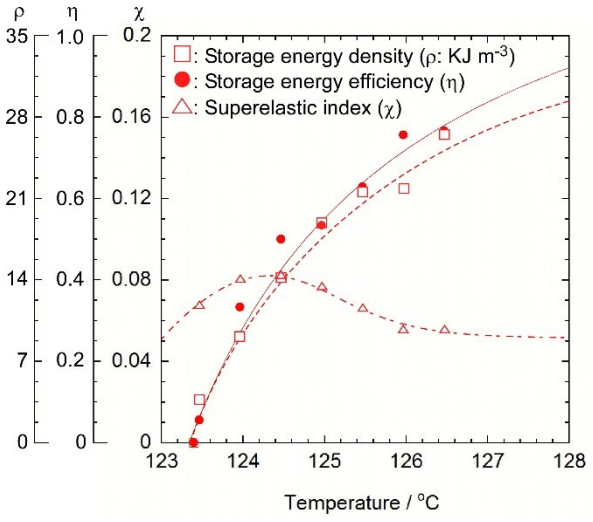

Figure S11. Temperature dependence of storage energy density (square), storage energy efficiency (solid circle), and superelastic index (triangle) in the superelastic region. The values are summarized in Table S3.

Single-Crystal Specimen for Heavy Lifting Work

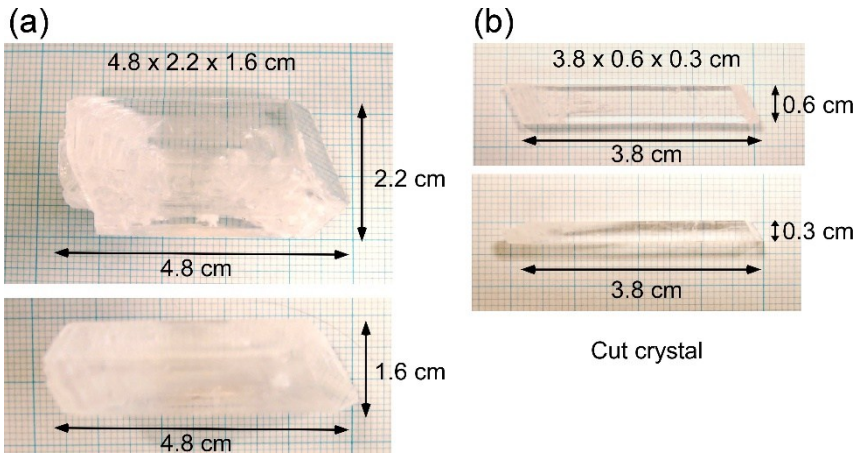

Figure S12. Photographs of a large single crystal of **1** (a) and a cut crystal for the lifting experiment (b).

View of Bending Crystal Specimens

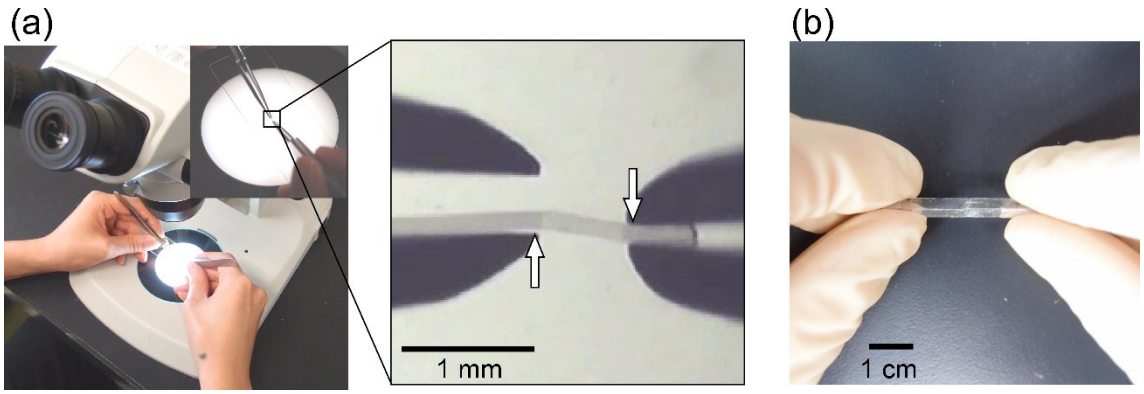

Figure S13. Typical procedures used to bend crystal specimens for small crystals (a) and large crystals (b). (The pictures clarify the experimental preparation for Fig. 1a and 1c (a) and in Fig. 7b (b).)